Applied Surface Science 475 (2019) 124–134

Contents lists available at ScienceDirect

Applied Surface Science

journal homepage: www.elsevier.com/locate/apsusc

Full Length Article

Molecular adsorption and surface formation reactions of HCl, H_2 and chlorosilanes on Si(100)-c(4 × 2) with applications for high purity silicon production

Shwetank Yadav[a], Chandra Veer Singh[a,b,*]

[a] Department of Materials Science and Engineering, University of Toronto, Canada
[b] Department of Mechanical and Industrial Engineering, University of Toronto, Canada

ARTICLE INFO

Keywords:
Hydrochlorination
Chlorosilane
Silicon tetrachloride
Trichlorosilane
Siemens process

ABSTRACT

The interaction of chlorosilanes and the silicon surface is an important part of reaction processes, such as hydrochlorination and chemical vapor deposition, involved in the production of high purity silicon. We used plane-wave based density functional theory (DFT) to investigate periodic slabs of the Si(100)-c(4 × 2) surface for adsorption of H_2, HCl, $SiCl_2$, dichlorosilane (SiH_2Cl_2 or DCS), trichlorosilane ($SiHCl_3$ or TCS) and silicon tetrachloride ($SiCl_4$ or STC). The effects of surface coverage, molecule orientation, adsorption site and multiple molecule adsorption were studied. All the molecules could undergo dissociative chemisorption in the right orientation and site placement, with HCl and $SiCl_2$ possessing the strongest binding energies. The H_2 molecule preferred lower coverage, the HCl molecule was not much affected by coverage while the $SiCl_2$ molecule strongly preferred higher coverage and the STC molecule was affected negatively by both too high or low coverage. The elementary steps leading to transfer of surface crystal silicon atoms to gas phase molecules as part of the chlorination or hydrochlorination process were then looked at through reaction pathway analysis. The formation of $SiCl_2$ from a surface dimer Si atom was found to prefer an intradimer route with a reaction barrier of 3.62 eV (83.48 kcal/mol), going down to 3.10 eV (71.49 kcal/mol) after removal of the first surface Si atom. The subsequent formation of TCS from this $SiCl_2$ was found to have reaction barrier of 1.07 eV (24.68 kcal/mol). STC could also be formed from this $SiCl_2$ molecule with a reaction barrier of 2.86 eV (65.95 kcal/mol).

1. Introduction

High purity silicon is essential for the production of both microelectronics and photo-voltaic (PV) solar cells. The strong recent growth in PV deployment and high expected future growth [1] has resulted in increased research focus on the manufacture of solar grade silicon in order to decrease costs and improve output. Metallurgical grade silicon (MG-Si), which has been obtained after ore processing, is typically further refined into solar grade (or the more stringent electronic grade) silicon through chemical processes in a number of energy intensive steps.

The majority of the world's solar grade silicon is produced by the Siemens process or its variants [2], which involves conversion of MG-Si to gaseous silicon based compounds which are distilled and then turned back to solid silicon through chemical vapor deposition (CVD). Both the first and last steps involve a two-phase chemically reactive system mostly consisting of chlorosilanes and hydrogen in the gas phase and a solid silicon surface [3]. Understanding the chemical interactions and reaction mechanisms of this system can help to improve modeling and optimization of the silicon refining process. *Ab initio* techniques provide an ideal tool to study this complex system for which there is still no consensus on the number and nature of elementary reactions.

The intermediate silicon compound used in the traditional Siemens process is trichlorosilane ($SiHCl_3$ or TCS). This is typically produced from MG-Si by treatment with HCl (often known as chlorination in industry) or silicon tetrachloride ($SiCl_4$ or STC) and H_2 (known as hydrochlorination), where the latter two produce HCl through a gas phase reaction:

$$SiCl_4(g) + H_2(g) \rightarrow SiHCl_3(g) + HCl(g) \quad (1)$$

The classic surface TCS production reaction is regarded as the following:

$$Si(s) + 3HCl(g) \rightarrow SiHCl_3(g) + H_2(g) \quad (2)$$

The reverse reactions happen during the CVD process, although

* Corresponding author at: 184 College St., Suite 140, Toronto, Ontario M5S 3E4, Canada.
E-mail address: chandraveer.singh@utoronto.ca (C.V. Singh).

https://doi.org/10.1016/j.apsusc.2018.12.253
Received 18 August 2018; Received in revised form 16 November 2018; Accepted 26 December 2018
Available online 27 December 2018

under different operating conditions. Looking at the above two simplistic reactions, one can speculate about the presence of other additional chemical species and reactions. Indeed, dozens of such elementary reactions and compounds involving the Si, Cl and H atoms have been proposed to be present in the gas phase for this system during CVD. Theoretical first principles based computational studies have taken the lead in such investigations as these techniques can easily study reactions which are difficult to isolate experimentally, are present in low proportion or consist of transient or fast reacting species.

Most papers focused on gas phase reactions in order to find enthalpies of formation and kinetic rate constants. These studies used quantum chemistry Gaussian-n composite methods involving Møller-Plesset (MP) perturbation theory and transition state or canonical variational transition state theory. An early study by Su et al. [4] studied thermal decomposition of monosilanes such as TCS and STC and obtained rate constants. Swihart and Carr continued the same thermal decomposition study with chlorinated disilanes [5] and followed up by looking at the thermal decomposition of TCS, dichlorosilane (SiH_2Cl_2 or DCS) and SiH_3Cl in hydrogen [6]. Several similar studies dealing with various decomposition reactions of silanes and chlorosilanes or their reactions with Cl, H or H_2 were also conducted [7–18].

In terms of forming a comprehensive reaction network with a large number of elementary reactions for the gas phase, Swihart and Carr [6] created a scheme of 39 elementary reactions using 20 different species. Ravasio et al. [19] came up with a 26 reaction and 16 species model, incorporating Swihart and Carr's disilane based mechanism with their own proposed radical chain mechanism. The most extensive network of reactions was proposed by Ran et al. [20], where the G3B3 method was used to study kinetics parameters for 117 reactions formed from 20 chemical species. Dkhissi et al. [21] compared DFT and composite quantum chemistry methods for compounds in a Si-Zn system where liquid Zn is used to reduce STC directly to Si(s).

There are very few computational atomic studies looking at gas-surface interactions and surface reactions. Due to the more expensive nature of modeling surfaces, these studies used density functional theory (DFT) but with atomic orbital basis sets which approximate surfaces as clusters of atoms. Hall et al. [22] had an early study looking at dissociative adsorption of multiple chlorosilanes (including TCS, DCS and SiH_3Cl) on the Si(100)-2 × 1 surface, predicting that DCS and TCS prefer to adsorb through Si—Cl bond cleavage rather than Si—H cleavage. DCS was found to have the lowest adsorption barrier and STC the highest (over three times higher). However, they only modeled a single dimer cluster consisting of 9 silicon atoms which differs significantly from a continuous surface.

Barbato and Cavallotti [23] looked at H_2 adsorption and desorption and H diffusion on a 7 seven layer 60–61 Si atom cluster (Si(100)-2 × 1 surface), with the latter two being conducted on both partially and fully hydrogenated surfaces. This involved studying 2H, 3H and 4H interdimer, an intradimer and two inter row (1H and 2H) desorption mechanisms (with xH representing the number of adsorbed H atoms on a pair of parallel dimers). The 1H inter row mechanism was found to have lowest activation energy. Cavalotti [24] also studied the Si(100)-2 × 1 surface for desorption of H_2 and HCl on 4 layer clusters of varying sizes up to 60 Si atoms. The 4H, 2H and intradimer mechanisms were tested for both species with 4H most favorable for H_2 and intradimer most favorable for HCl.

Kunioshi et al. [25] looked at adsorption and desorption of H_2 and HCl on the Si(100)-2 × 1 surface with 4 layer clusters. They varied the size of clusters by the number of dimers (the largest cluster having six dimers), investigating parallel and adjacent dimers and found that parallel clusters were needed to give converged adsorption energies. They found H_2 adsorption proceeds through intradimer mechanism while desorption might occur by 3H or 4H mechanisms. HCl adsorption had almost zero or negative barriers and desorption proceeded through intradimer mechanism. Anzai et al. [26] looked at $SiCl_2$ adsorption, desorption and diffusion on the same cluster system. They looked at both interdimer and intradimer sites and multiple molecule adsorption adjacent to each other. They did not find dissociative adsorption of $SiCl_2$ as had been predicted in some earlier silicon epitaxial growth kinetic models.

Beyond adsorption, two key processes which form part of reaction (2) are the removal of bulk silicon atoms from the solid surface (in effect etching the surface) and formation of TCS on the surface before its desorption. The mechanisms for these steps have not been much studied by simulations. Valente et al. [27] came up with a set of surface reactions, including two involving bulk Si atoms. They relied on previous studies and their own work by which they gathered kinetic parameters based on collision theory, experimental data fitting and semi-empirical methods. They claimed to verify the most relevant reactions through quantum chemistry calculations using first semi-empirical methods such as PM3 and then DFT, while specifically mentioning only the HCl desorption reaction (studied through PM3). Their two bulk Si atom reactions have activation energies derived from the experimental work of Gupta et al. [28] and do not seem to have had any further *ab initio* calculations applied as their energies are exactly the same as the experimental values and identical for both reactions. Furthermore, the experimental value supplied by Gupta et al. is derived from $SiCl_2$ desorption following earlier adsorption and saturation of the surface by STC. Hence, there do not appear to be any simulation of reactions involving bulk silicon atoms and surface etching in the literature.

The Si(100) surface is well known to undergo surface reconstruction whereby undercoordinated surface Si atoms join together in pairs to form dimers. Several dimer reconstructions have been theorized and observed, although there is some debate about the nature of experimentally observed reconstructions at different temperatures or frequency of occurrence. Some might be misidentified due to artifacts introduced by the electron microscopy equipment or flipping of dimers [29]. Regardless, the symmetric p(2 × 1) and buckled c(4 × 2) reconstructions have been regarded as having the lowest energies which differ very little in value. Different computational techniques have either suggested the symmetric or buckled dimers as more stable, although higher accuracy techniques better at dealing with electron correlation effects predict buckled dimers as more stable [30]. Guo et al. [29] have recently provided theoretical simulations which support experimental evidence that the c(4 × 2) reconstruction is the most dominant and stable (resistant to dimer flipping) at room temperature.

As pointed out earlier, the few *ab initio* surface simulations of the chlorosilanes based system for TCS formation from solid silicon were conducted using clusters which do not simulate continuous surfaces. As this crystalline structure is one of the key characteristics differentiating a surface from molecules in the gas phase, it is important to use a computational technique which can capture its long range effects. Plane wave based DFT is ideally suited for such a task as it simulates periodic slabs with unbroken surfaces and can handle larger numbers of atoms. Hence, this study aimed to look at the interaction of chlorosilane species with the Si100 c4 × 2 reconstruction using a periodic slab model. The adsorption of multiple species (H_2, HCl, DCS, TCS, STC and $SiCl_2$) was investigated in a single study at the same level of theory while including the effects of surface coverage. Subsequently, the formation of surface TCS and STC from bulk Si atoms was found through two elementary reactions steps along with their activation energies, which we believe is the first *ab initio* study of such reactions in the literature.

2. Methodology

The simulations were performed using plane wave based DFT as implemented in the Quantum Espresso software [31]. Interactions between the valence electrons and the ionic core were represented by the projector augmented wave (PAW) [32] method with Perdew-Burke-Ernzerhof (PBE) formulation [33]. Kinetic energy cutoffs of 680 eV (50 Ry) and 3400 eV (250 Ry) were used for the wave functions and the

charge density, respectively. Brillouin zone integrations were performed using a Monkhorst-Pack [34] grid of 2× 4× 1 k-points and all calculations were non spin polarized. A vacuum layer of 15 Å, based on iterative testing, was added to avoid interaction between periodic surface images. Each slab was 7 layers thick with the bottom of the slab being hydrogen terminated. The structures were relaxed using a Davidson minimization algorithm until the magnitude of the residual Hellman-Feynman force on each atom was less than 0.025 eV $Å^{-1}$.

The evaluation of minimum energy reaction paths (MEPs) and transition states (TS) was performed using the climbing image nudged elastic-band (CI-NEB) method [35–37]. Each pathway was sampled with a minimum of five images. Finite temperature analysis of certain systems at 873 K was conducted through ab initio molecular dynamics (AIMD) on the Born–Oppenheimer surface which maintained temperature through the Andersen thermostat. A time step of 1.0 fs was employed for the AIMD runs, wherein Brillouin zone integrations were performed on the same grid of 2× 4× 1 k-points. Zero-point energy corrections and Helmholtz free energies were calculated using the harmonic limit model as implemented in the atomic simulation environment (ASE) software package [38].

The basic supercell used for all simulations, except those using larger supercells for coverage studies, is shown in Fig. 1. This can be regarded as a unit cell which contains the four dimers required to define a c(4 × 2) reconstruction on the Si(100) surface.

Table 1
Adsorption energies (eV) for single molecules (H_2, HCl, $SiCl_2$, DCS, TCS and STC) on the Si(1 0 0) c(4 × 2) surface for various sites.

Site	H_2	HCl	$SiCl_2$	DCS	TCS	STC
Top	−1.829	−2.478	−1.383 (∥ to surf.)	−1.744	−1.764	−1.794
Mid	0.010	−0.152	−1.369	−0.036	−0.005	−0.016
Interdimer	0.010	−2.960	−1.972	–	–	–
Intradimer	–	–	−2.114 (⊥ to surf.)	–	–	–

3. Results and discussion

3.1. Single molecule surface interaction

Each molecule was first tested for adsorption by placement at two sites over the surface and allowing for structural relaxation (see Fig. 1 for sites). The ‘top’ site corresponded to being placed over a dimer and placed molecules closer to the surface Si atom with the most exposed charge available for interaction (the atom in each dimer furthest from the bulk structure). The ‘mid’ site corresponded to being placed equidistant from all four dimers over a region directly exposed to the second layer under the surface. Depending on the results and nature of the adsorbent molecule, subsequent sites or orientations (such as intra and interdimer) were then tested. The resulting adsorption energies are

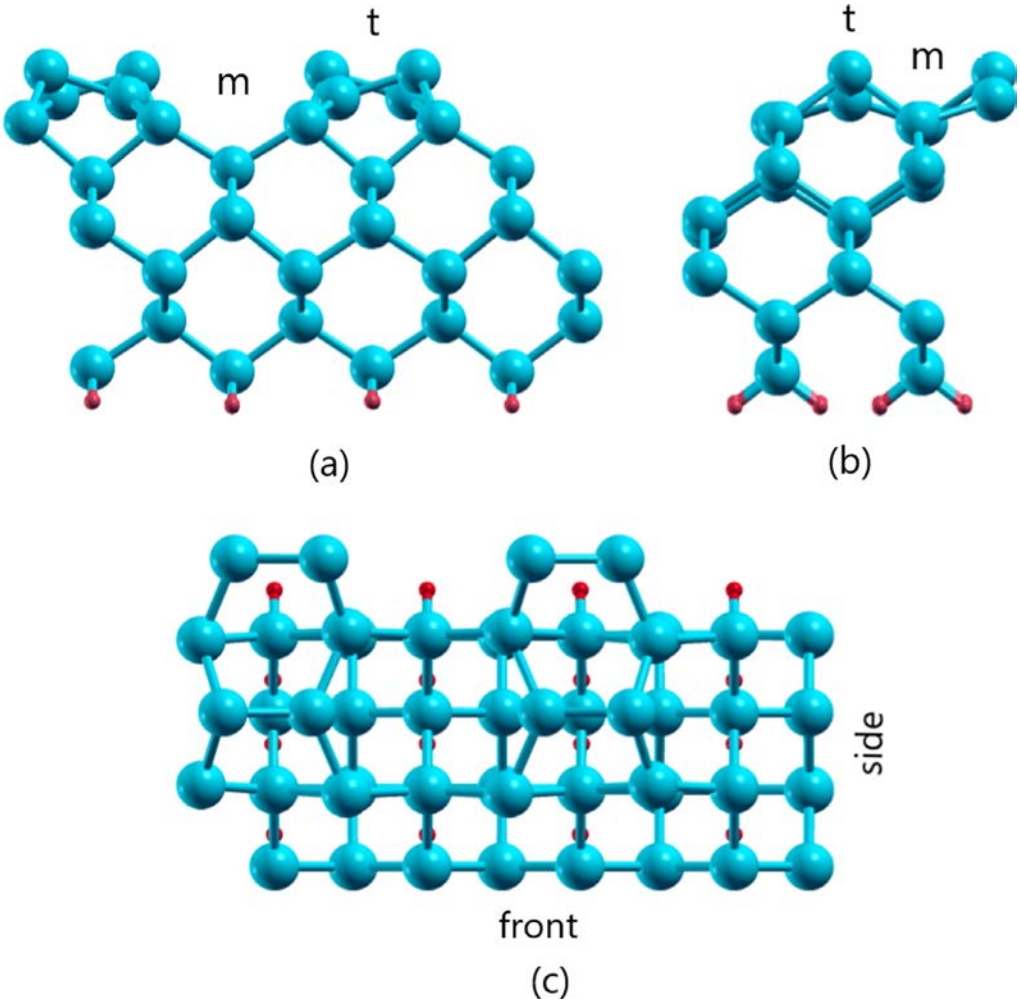

Fig. 1. Front (a), side (b) and top (c) views of the supercell used for all simulations (other than low surface coverage tests). This is the smallest sized cell containing all four dimers required to reproduce the c(4 × 2) reconstruction. Blue atoms are Si and red atoms are H. The ‘t’ (top) and ‘m’ (mid) labels indicate sites for molecule placement.

presented in Table 1. All atoms below the third layer of the surface were frozen during relaxation to simulate effects of a bulk structure. Note that the adsorption energy simulations did not test any adsorption barrier which may exist to bring molecules from free gas like state (for instance over 5 Å away) to the surface, but rather what occurs if the intact molecule is placed within 2.0 Å of the surface. After finding the best adsorption site of each molecule, the adsorption barrier from gas phase was calculated using CI-NEB and is presented in Table 3.

The adsorption (or binding) energy of a molecule on the surface was calculated as:

$$\Delta E_{ads} = E_{tot} - E_{bare} - E_{ad}, \quad (3)$$

where E_{tot} (E_{bare}) are the energy of the slab with (without) adsorbate and E_{ad} is the energy of the isolated adsorbate species calculated in the same supercell. Hence, a negative ΔE_{ads} indicates stable adsorption whereas a positive value indicates unstable adsorption, with a more negative value indicating more favorable adsorption.

Both H_2 and HCl, diatomic molecules having the same geometry, strongly adsorbed over the top site where they had been placed parallel to the underlying dimer, with HCl being more favorable by a significant margin. In fact, both of these molecules underwent intradimer dissociative chemisorption with no energy barrier as can be seen in Fig. 2. In contrast, Cavallotti [24] and Kunioshi et al. [25] found that H_2 adsorption has an adsorption barrier of 0.75–0.78 eV, although this decreases with larger clusters and a greater number of parallel dimers. They did find close to zero or slightly negative barriers for HCl adsorption, still far less favorable then the 2.5 eV drop in energy observed in our simulations. This might hint at the effect of having a continuous slab, not having nearby H atoms for passivation (which are found even at top edges for previously simulated clusters versus only bottom of the slab for our simulations) or the stabilizing effect of nearby periodic molecules (although as the next sections shows, increasing the distance to nearby molecules does not affect binding energies much for these two molecules). Another factor may be the use of different functionals, as the previous studies used B3LYP hybrid functionals, with Cavallotti pointing out that the plane wave PW91 functional can underestimate reaction energies by 0.43 eV compared to B3LYP (though B3LYP has been found to degrade in formation energy prediction with increasing system size [39]). Furthermore, different possible starting positions of the molecules might have been used. The previous simulations might have started from an energy well which was separated from the surface by a larger barrier, possibly due to a larger distance from the surface.

Dissociation did not take place for the 'mid' site tests, where the HCl molecule was physisorbed (with a low binding energy) and the H_2 molecule did not show any preference for adsorption as it moved away from the surface during relaxation. This difference could be due to the smaller radius of the H atom in comparison to the Cl atom, leading to less likely and weaker interaction with surrounding Si surface atoms as well the fact that the HCl molecule is far more polar. The molecules were also tested for interdimer adsorption by placing them between two parallel dimers, perpendicular to each dimer. The H_2 molecule again moved away from the surface while the HCl molecule had an even stronger dissociative adsorption energy than for the intradimer mechanism of the 'top' site. The interdimer adsorption (Fig. 2(c)) might produce a more stable system as each adsorbed atom has two adjacent adsorbed atoms on the parallel dimers on either side. Cavallotti [24] also reported activation barriers for interdimer adsorption of both molecules, with HCl being more favorable (having barriers varying from 0.09 eV to 0.35 for 4H and 2H interdimer mechanisms).

The $SiCl_2$ molecule is theorized to play an intermediate species role in most proposed mechanisms and is a natural (and relatively stable) sub-unit of the larger 5 atom molecules common in the reacting system. Adsorption energies for the four tested configurations are shown in Table 1, where each of them underwent chemisorption. Such strong interaction is explained by the under-coordinated nature of the molecule where the Si atom has two bonds compared to its preferred four bond arrangement. The molecule was fist placed in the 'top' and 'mid' positions in an orientation where it was parallel to the surface and dissociatively adsorbed by interdimer mechanism (splitting across two parallel dimers) for both cases (See Supporting Information (SI) for a more detailed geometry). The $SiCl_2$ molecule was next tested by placement at the 'top' position perpendicular to the dimer (Fig. 3(a)) where it retained it's integrity and orientation while forming bonds with each of the dimer's two atoms in a triangle intradimer configuration (Fig. 3(b) and (c)). This geometry and a somewhat close (no barrier) adsorption value of 1.839 eV was also obtained by Anzai et al. [26]. Finally, the molecule was placed between two parallel dimers, perpendicular to each dimer and the surface, to test adsorption from an interdimer position. The molecule again retained its integrety and formed bonds to two surface silicon atoms similar to the intradimer position, though with a different orientation. Note that Anzai et al. claim that $SiCl_2$ does not adsorb dissociatively as has been proposed in certain recent kinetic schemes. However, our results show that if $SiCl_2$ approaches the surface at the right orientation (parallel to the surface), it can indeed dissociate into SiCl and Cl. The charge density difference plot and PDOS for intradimer adsorption (the strongest binding energy) is show in in Fig. 3(d) and (e), demonstrating a strong covalent character as there is no clear charge polarization between atoms and there is overlap between atomic orbital occupancies of all atoms.

The DCS, TCS and STC molecules have fully coordinated (fourfold) Si atoms in their centers, resulting in more stable molecules. As such, these molecules usually remained intact and moved away from the surface during relaxation with positive or barely negative binding energies for both 'mid' and 'top' sites. However, when the molecules were orientated to have the center silicon atom directly above a silicon atom in a dimer pair with a chlorine atom over the other silicon atom of the dimer, and placed close to the surface (around 2.5 Å), they underwent dissociative chemisorption (Fig. 4). This proceeded by Si−Cl bond cleavage in the molecule, which was reported by Hall et al. [22] to be the lowest barrier dissociation route and the motivation for orienting a

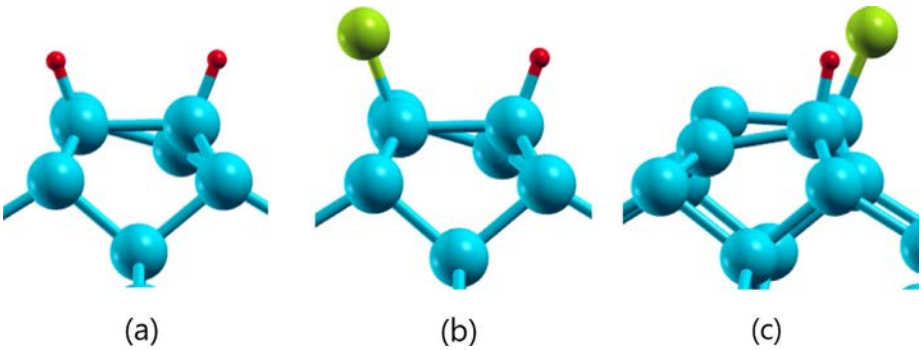

Fig. 2. Dissociative intradimer adsorption of (a) H_2 and (b) HCl over a dimer at the 'top' site. Dissociative interdimer adsorption of HCl (c) over two parallel dimers. Blue atoms are Si, yellow are Cl and red are H.

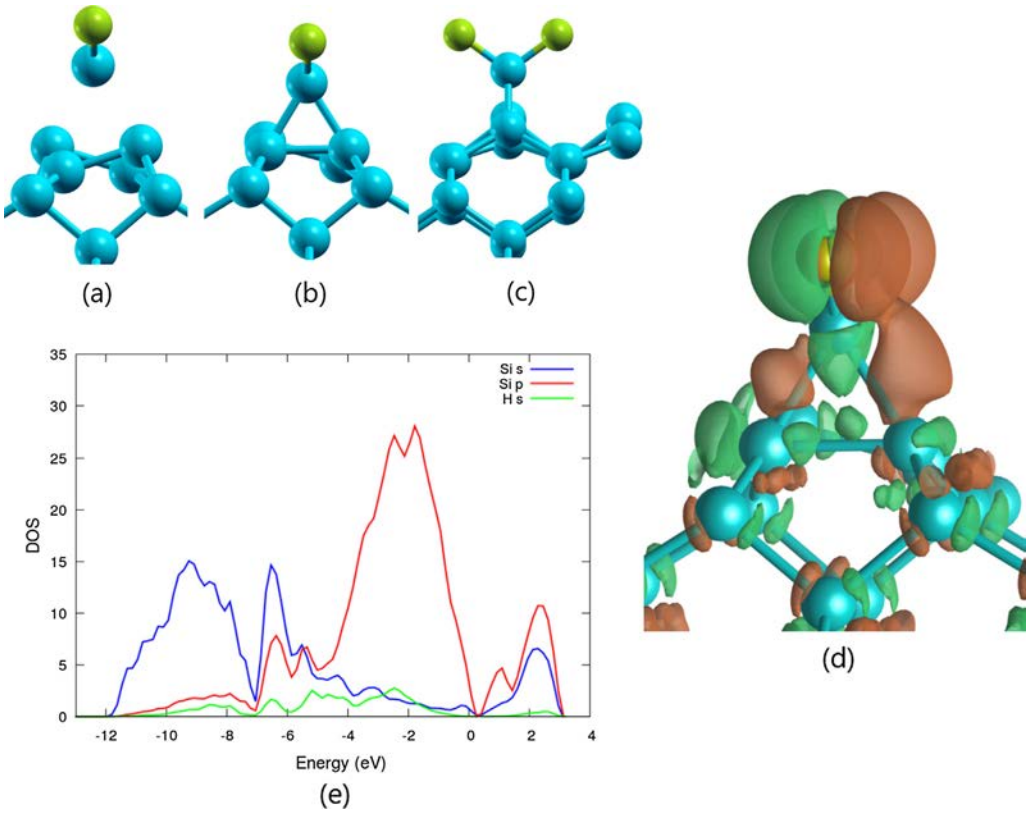

Fig. 3. Intradimer adsorption of $SiCl_2$ at the 'top' site. Initial orientation (perpendicular to surface) of $SiCl_2$ molecule (a). Final adsorbed state, front (b) and side (c) views. The charge density difference (d) and PDOS (e) are representative of typical strong covalent bonding and charge sharing. For the PDOS, green regions indicate charge loss while brown indicates charge gain.

Si−Cl bond from each molecule directly above the dimer. The resulting strong adsorption energies (see Table 1) were all similar in value (with STC being most favorable for adsorption) but still weaker than those for all the smaller tested molecules. This dissociative adsorption ability of the STC molecule was then tested for finite temperature conditions through AIMD at 873 K where it indeed dissociated and split after 1.24 ps, indicating a spontaneous reaction (see SI for geometry).

3.2. Surface coverage and multiple molecule adsorption

The effect of surface coverage, the fraction of surface sites covered with adsorbates, relates to the distance between adjacent adsorbed molecules. For lower coverage, the original supercell was doubled in size along the narrower dimension (the side edge in Fig. 1), effectively halving surface coverage for a single molecule adsorbed at the same position used for previous simulations (see Fig. 5). This had an additional impact of increasing the distance between periodic molecule images along the side edge which had been previously separated by about 8 Å (compared to around 15 Å along the front edge) and could have been a source of molecular interaction and stabilization. The now doubled supercell resulted in periodic molecule images being separated by a distance of at least around 15 Å in each direction, which should have resulted in almost no interaction effects as this was also the vacuum spacing over the slab. Note if each dimer is regarded as an adsorption site for a molecule, then full coverage would have a molecule adsorbed on each dimer.

For lower surface coverage, the 'top' site was tested again for each of the three molecules which adsorbed regardless of orientation (H_2, HCl and $SiCl_2$) and STC (to represent the larger molecules and as the molecule of most interest to adsorb as part of the hydrochorination process). The adsorption energies are given in Table 2. The energies for H_2 and HCl were barely changed from the smaller supercell results, being slightly more favorable, and both dissociatively adsorbed into the same geometry. This removes the possibility of periodic molecular image

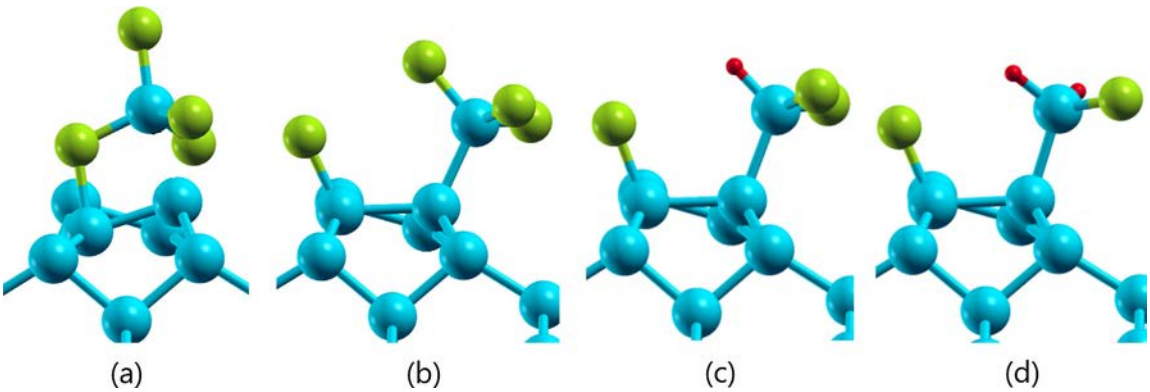

Fig. 4. Adsorption of the larger five atom molecules at the 'top' site. Initial orientation required to produce dissociative chemisorption for each molecule (a) (STC shown as example). Final adsorbed state of STC (b), DCS (c) and TCS (d).

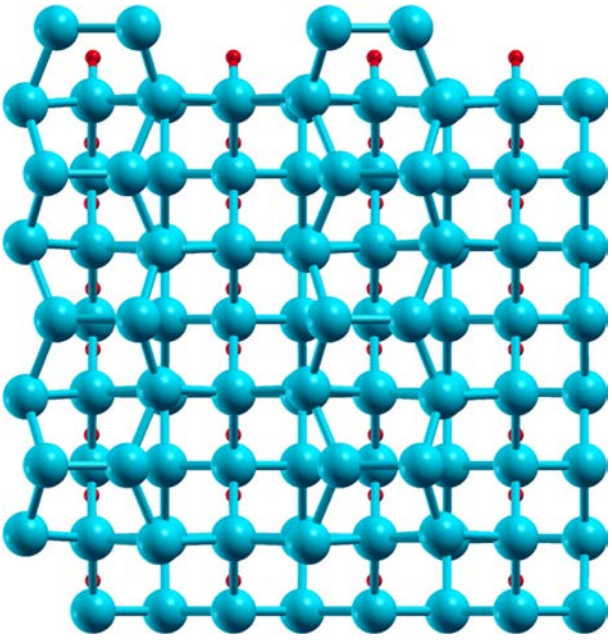

Fig. 5. The increased size supercell used to test low coverage effects, top view. The original supercell has been doubled in size along the side edge in Fig. 1, with 8 surface dimers now present. The length along the front edge and the depth remain the same. This effectively halves surface coverage when single molecules are adsorbed.

Table 2
Adsorption energies (eV) of molecules over 'top' site dimers for varying surface coverages. The lowest surface coverage is provided by doubling the original supercell while increased coverage is provided by adsorbing additional molecules in the original supercell. Each surface dimer is regarded as a single adsorption site with full coverage defined as one molecule adsorbed per dimer.

No. of molecules	Coverage	New molecule	Average per molecule
		H_2	
1 (double cell)	0.125	−1.853	−1.853
1	0.25	−1.829	−1.829
2	0.50	−0.008	−0.918
		HCl	
1 (double cell)	0.125	−2.503	−2.503
1	0.25	−2.478	−2.478
2	0.50	−2.515	−2.497
3	0.75	−2.567	−2.520
4	1.00	−2.495	−2.514
		$SiCl_2$	
1 (double cell)	0.125	−0.970	−0.970
1	0.25	−1.383	−1.383
2 (intradimer)	0.50	−2.876	−2.130
2 (new clean surf.)	0.50	–	−2.715
		STC	
1 (double cell)	0.125	−1.475	−1.475
1	0.25	−1.794	−1.794
2	0.50	−0.917	−1.355

interaction being a cause for the stronger adsorption in our results in comparison to cluster based studies.

The $SiCl_2$ molecule did present a change in adsorption energy, although it still displays chemisorption, and does not dissociate as in the smaller supercell results. Instead the molecule rotates from its initial parallel orientation to adsorb to a single Si dimer atom at an orientation between parallel and perpendicular to the surface. This indicates that the adjacent periodic $SiCl_2$ molecules in the original supercell did help stabilize the dissociation. The STC molecule also saw a decrease in adsorption energy, similarly indicating stabilization effects, but did still undergo dissociation into the same geometries.

Higher surface coverage was tested next by adding a second molecule to the original supercell over a similar 'top' type site (with a total of four dimers and hence four 'top' sites available in the supercell), effectively doubling surface coverage. This molecule was placed over the dimer in the corner of the supercell opposite to which the first molecule had been placed, thus helping to keep maximum separation between adsorbed molecules. For H_2, the second molecule did not dissociate and moved away from the surface to end up with a slightly negative binding energy. This clearly shows the H_2 molecule does not have very strong interactions with surface atoms or molecules further away. In fact, the presence of other H_2 molecules seems to be not beneficial as adsorption energies decrease with increasing coverage (Table 2). Additional molecules did not produce negative binding energies.

For HCl, the second molecule also dissociatively adsorbed in the same manner as the first, with roughly the same but slightly more favorable adsorption energy (Table 2). Subsequent molecules were added until all four dimers had dissociatively adsorbed molecules (see Fig. 6(a)), producing a coverage four times higher than the original simulation in Section 3.1. The adsorption energy of each additional molecule hardly changed, resulting in a mostly steady average adsorption energy per molecule of HCl, staying within 0.1 eV of each other. There was no obvious pattern in energy change with additional molecules as adsorption energies first decreased and then increased, although all multiple adsorption energies were slightly more favorable than a single molecule. The seemingly spontaneous nature of the HCl molecule dissociations was tested for finite temperature conditions through AIMD at 873 K where it indeed dissociated and split after 0.25 ps, indicating a spontaneous reaction (see SI for geometry). The charge density difference plot and PDOS for the fourth molecule adsorption is show in Fig. 6(b) and (c). The charge density difference is between the final adsorbed state and an initial state where the HCl molecule was hovering over the site, showing that most of the charge of the adsorbed atoms was from their original molecule (with a slight amount moving from the dimer bond towards the adsorbed atoms). The previous adsorbed atoms show typical covalent bond character as there is no clear charge polarization between atoms. The PDOS further confirms the strong covalent nature of bonds due to overlap between atomic orbital occupancies of all atoms.

The $SiCl_2$ molecule presented a more complex situation for multiple molecule adsorption as it had more orientation possibilities. The five different higher coverage configurations tested are described in detail in terms of energies and their complex geometries in the SI while the two strongest binding configurations are presented in Table 2. The addition of a second molecule through intradimer adsorption led to much stronger binding energies, once again hinting at the strong stabilization effects for the $SiCl_2$ molecule (all tested configurations produced stronger average binding energies after adding a second molecule). However, the addition of two new molecules simultaneously on a clean surface (placed adjacent to each other on two parallel dimers) produced an even stronger average binding energy, in fact the strongest of all coverage simulations. This likely results from the strong interaction and arrangement the two molecules were able to undergo, something not possible if an earlier molecule had adsorbed as that would have rotated to present a geometry not allowing the same approach of a second molecule onto a parallel dimer.

Finally, a second STC molecule was able to dissociatively adsorb on the dimer in the opposite corner from the first (other dimers could not be tested due to geometric constraints, as can be seen in SI). The adsorption of the second molecule was markedly less favorable, having half the strength of the first (Table 2), although average adsorption energy did not decrease by much. This is likely related to the fact that the large $SiCl_3$ clusters from both molecules underwent rotation and positional adjustment in relation to each other, hinting at a strong interaction between the two and settling into a shared low energy

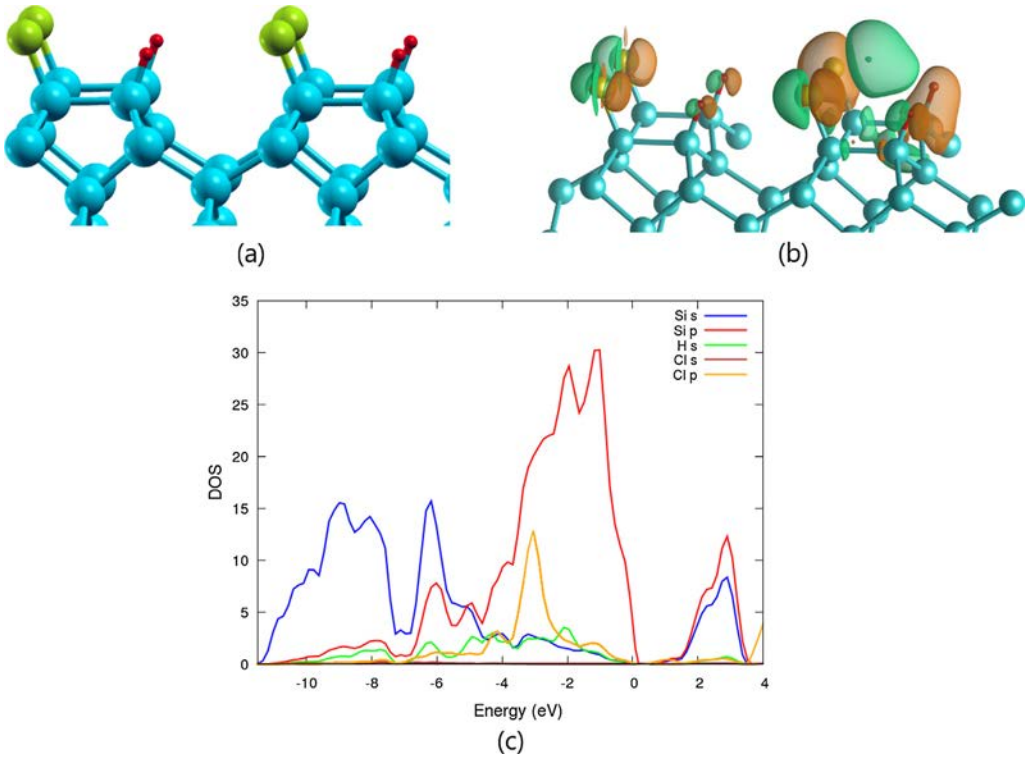

Fig. 6. The dissociative adsorption of four HCl molecules (a) on all available surface dimers, representing the maximum surface coverage obtained in this study. The charge density difference (b) and PDOS (c) are representative of typical strong covalent bonding. For the PDOS, green regions indicate charge loss while brown indicates charge gain.

configuration.

3.3. $SiCl_2$ formation from surface silicon

The primary purpose of silicon hydrochlorination is to remove silicon from the solid phase to gas phase. A straightforward route would be for surface Si(s) to become part of an adsorbed species which travels to the gas phase through desorption. According to reaction (2), the eventual molecule which desorbs to gas phase is TCS. However, direct movement of a Si atom which is part of the crystalline structure to a fully formed large molecule like TCS is likely to be very unfavorable. Rather, it is likely the Si (s) atom becomes part of an intermediate species before forming part of the TCS molecule. One such likely candidate is the $SiCl_2$ molecule, which can be formed from the surface Si atom in a dimer (the dimer Si atoms are most likely candidates by which the surface would be eroded) and adsorbed Cl atoms. The Cl atoms themselves would be provided by adsorption of HCl, which as shown previously, readily attaches to the dimers. The following reaction was then tested through NEB:

$$2Cl^* + Si(s) \rightarrow SiCl_2^* \quad (4)$$

This was tested through two possible routes, an intradimer mechanism where the Cl atoms were adsorbed on the same dimer and an interdimer mechanism where the two Cl atoms were adsorbed on parallel dimers. The configuration of two Cl atoms on the same dimer could be achieved by two interdimer adsorptions of HCl while two Cl atoms on parallel dimers could be achieved by intradimer adsorption on the 'top' position as shown in Section 3.1. The required rearrangement of surface atoms could also occur through surface diffusion of atoms. Both routes were tested with and without the remaining dimer atoms, which were not participating in the reaction, also having adsorbed atoms to see any stabilization effects of adsorbate interactions. The presence of an additional HCl molecule helped for the intradimer route while the interdimer route preferred no secondary adsorbates.

The intradimer route (Fig. 7) was found to have a lower barrier of 3.62 eV (83.48 kcal/mol) as seen in Table 3 with the highest energy transition state only slightly higher energy than the final state in which the formed $SiCl_2$ molecule adsorbed onto the remaining Si atom of the dimer. The interdimer route was found to have no transition state and would spontaneously decompose upon convergence and so was not studied further. Note that the final state of the intradimer route now has all the five atoms required to form a TCS molecule adsorbed in the same region. After one $SiCl_2$ molecule had been formed, the ability to form a second $SiCl_2$ molecule from a bulk Si atom was tested.

A Si atom from the adjacent parallel dimer was able to form $SiCl_2$ with a lower activation barrier of 3.10 eV (71.49 kcal/mol), although the reverse reaction had a very small activation barrier (see SI). When the remaining Si atom of the original dimer was tested, the $SiCl_2$ molecule decomposed into a physisorbed SiCl unit and Cl upon convergence. Note that these barriers were higher than the assumed 2.91 eV (67 kcal/mol) of Valente et al. [27] derived from experimental desorption of $SiCl_2$ by Gupta et al. [28]. The latter's results were stated to have an error of ± 0.22 (5 kcal/mol), bringing the higher range of their experiment derived barrier to 3.13 eV. Hence, our computed barrier for $SiCl_2$ formation after an initial Si atom had been removed (expected to more closely match the average barrier deduced in experiments as surface atoms are continuously removed) are reasonably close in matching these earlier experimental derived kinetic parameters.

3.4. TCS formation

As discussed in the previous section, TCS formation from a surface Si (s) atom is likely to proceed through an intermediate species and one such logical species is $SiCl_2$. The formation reaction is then likely to occur when all constituent reactants are adsorbed on the surface in close proximity, most likely on the sites of two parallel dimers. The intradimer route for $SiCl_2$ formation has such a final state with an adsorbed $SiCl_2$ molecule over the remaining Si atom of the dimer (which supplied it's Si atom) and H and Cl atoms adsorbed on the parallel dimer (Fig. 7). Hence, this was used as a starting point for studying TCS formation routes. The most straightforward mechanism involves the Si atom of the $SiCl_2$ forming the center atom of the TCS molecule with the adsorbed H and Cl simply forming bonds to the Si atom of the $SiCl_2$ to

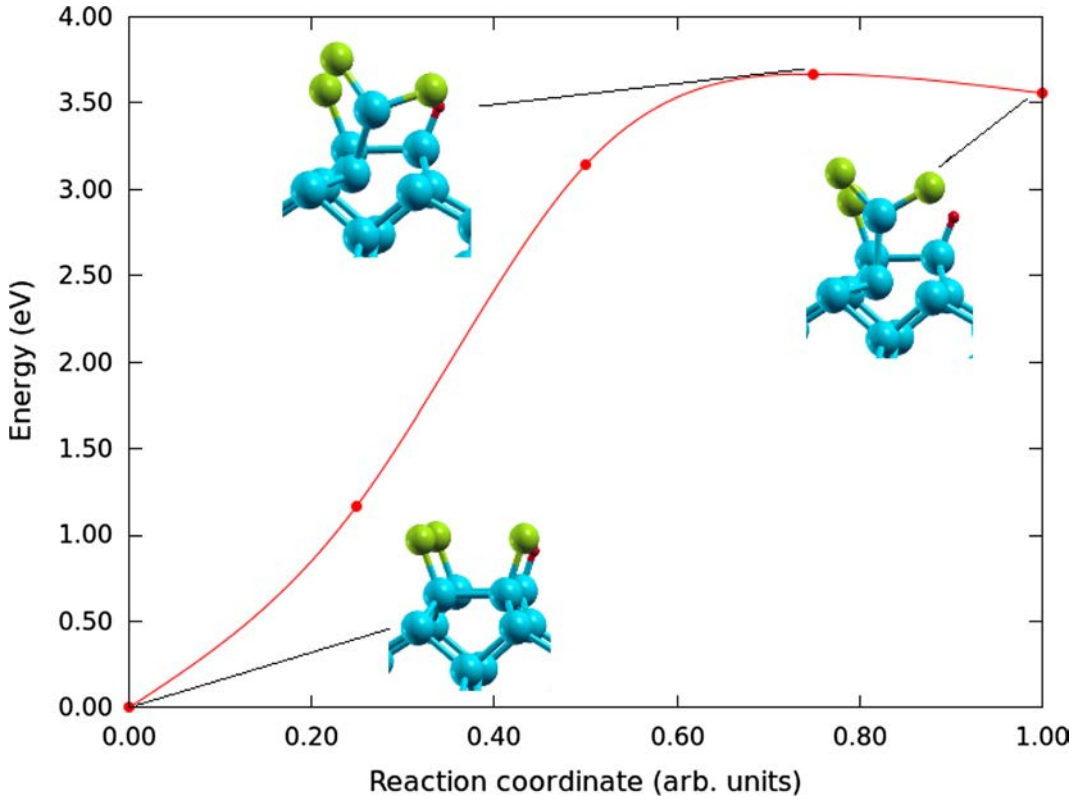

Fig. 7. Reaction pathway for the formation of a $SiCl_2$ molecule from a surface dimer Si (s) atom and two Cl atoms adsorbed on the same dimer in an 'intradimer' route. The reaction barrier was found to be 3.67 (84.63 kcal/mol), producing a free energy barrier of 3.62 eV (83.48 kcal/mol). The presence of an adsorbed HCl molecule on the parallel dimer was found to slightly decrease the barrier.

complete the molecule. The reaction would be represented by the following equation:

$$SiCl_2^* + Cl^* + H^* \rightarrow SiHCl_3 \quad (5)$$

Two possible routes were investigated whereby the $SiCl_2$ approached the H and Cl atoms. The first involved the $SiCl_2$ rotating to have all three atoms in a plane perpendicular to the surface plane and approaching the mid-point of the adsorbed H and Cl atoms with the Si atom leading, whereby it would bond with both atoms in place and have roughly the shape of the fully formed TCS molecule. The second route involved $SiCl_2$ molecule rotating to have all three atoms parallel to the surface and approach adsorbed H and Cl atoms with Si atom leading again and would now require the H and Cl atoms to move and bond to the Si atom to form the TCS molecule shape. The appropiately rotated $SiCl_2$ molecule was supplied as an intermediate image guess for both pathways in the NEB simulation setup. Upon convergence, both routes produced the same barrier of 1.07 eV (24.68 kcal/mol), with the second route's intermediate image eventually rotating to an intermediate geometry similar to the first route. Therefore, the pathway for only the first route is provided (Fig. 8) with the second route being virtually identical with similar transition states. This is quite a low energy barrier and clearly illustrates that $SiCl_2$ formation would be the limiting reaction in the process of removing surface silicon to gas phase in the form of TCS.

A direct route from bulk Si to the desorbed TCS molecule was also tested with initial intermediate images from the above TCS formation route and with the formed $SiCl_2$ molecule (Fig. 9). This direct one-step path converged to an activation barrier of 4.92 eV (113.46 kcal/mol). The transition state for this latter path corresponds to one of the images on the earlier presented $SiCl_2$ to TCS path, being the next image after the transition state on the earlier path. This is not surprising as these two images are very close in energy in this earlier path (Fig. 7). On the other hand, if one even simply adds the activation barriers of the separate $SiCl_2$ and TCS formation steps then one gets 4.69 eV or 4.64 eV if adding to the final energy of the $SiCl_2$ formation step. This might indicate that the path to final desorbed molecule from initial adsorbed H

Table 3
Surface reactions with their activation barriers for forwards ($E_{a(f)}$) and reverse ($E_{a(r)}$) directions, reaction energies (ΔE_{rxn}) and free energy activation barrier for the forward direction at 300 K ($F_{a(f)}$). Here $*$ denotes a surface site, (g) denotes a molecule away from the surface representing gas phase and (b) denotes bulk phase. All energies are in eV.

Reaction		$E_{a(f)}$	$E_{a(r)}$	ΔE_{rxn}	$F_{a(f)}$
STC ads	$SiCl_4(g) + 2* \rightarrow Cl* + SiCl_3*$	0.27	2.14	−1.87	0.0
DCS ads	$SiH_2Cl_2(g) + 2* \rightarrow Cl* + SiH_2Cl*$	0.0	1.76	−1.76	0.0
TCS ads	$SiHCl_3(g) + 2* \rightarrow Cl* + SiHCl_2*$	0.17	1.94	−1.77	0.05
$SiCl_2$ from bulk Si (no bulk atoms removed)	$Si(b) + 2Cl* \rightarrow SiCl_2*$	3.67	0.11	3.56	3.62
$SiCl_2$ from bulk Si (after one bulk atom removed)	$Si(b) + 2Cl* \rightarrow SiCl_2*$	3.21	0.01	3.20	3.10
TCS formation from $SiCl_2$	$SiCl_2* + Cl* + H* \rightarrow SiHCl_3(g)$	1.08	0.22	0.86	1.07
TCS formation direct from bulk Si	$SiCl_2* + Cl* + H* \rightarrow SiHCl_3(g)$	5.10	0.60	4.50	4.92
STC formation	$SiCl_2* + 2Cl* \rightarrow SiCl_4(g)$	2.87	1.01	1.23	2.86

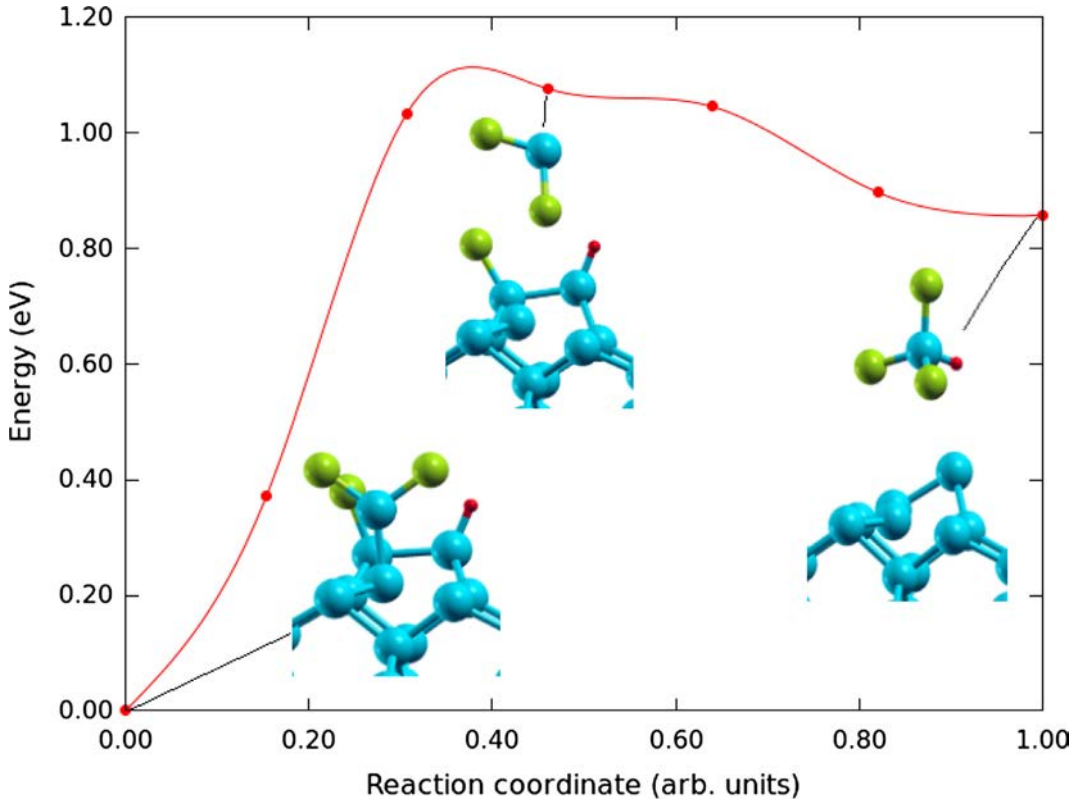

Fig. 8. Reaction pathway for the formation of a TCS molecule from $SiCl_2$, H and Cl adsorbed on parallel dimers. The reaction barrier was found to be 1.08 eV (24.91 kcal/mol), producing a free energy barrier of 1.07 eV (24.68 kcal/mol) at 300 K. The $SiCl_2$ had been previously formed from a surface dimer Si (s) atom, Fig. 7.

and Cl atoms is not linear in which case it is not well described by NEB. Then breaking this path into two steps would help better capture minimum energy path. As initial and final images were also allowed to relax, there might also be some states or movement not captured between the final image of the $SiCl_2$ formation step and initial imiage of the TCS formation step but which were accounted for in the direct one step path. One can conclude that the barrier to form a desorbed TCS molecule from a bulk silicon atom is likely between 4.69–4.92 eV with

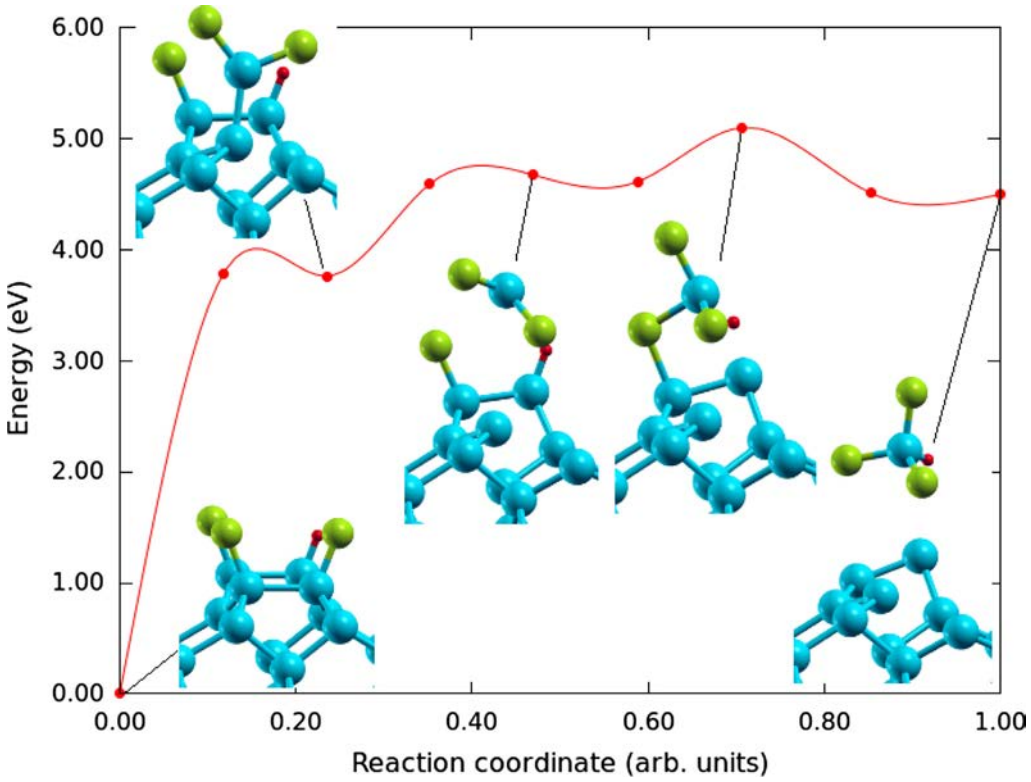

Fig. 9. Reaction pathway for the direction one-stage formation of a TCS molecule from a bulk surface dimer Si (s) atom and two Cl atoms adsorbed on the same dimer. The activation barrier was found to be 5.10 eV (117.6 kcal/mol), producing a free energy barrier of 4.92 eV (113.46 kcal/mol) at 300 K. The two-stage $SiCl_2$ and then TCS formation path overall follows almost the same geometries but with lower energies.

strong confidence on the upper limit.

3.5. STC formation

The STC molecule can be formed from the TCS molecule by switching the latter's H atom with a Cl atom and both molecules have a similar geometry. The initial state of the TCS formation reaction in the previous section therefore provides a straightforward starting place for forming STC if the adsorbed H atom is replaced with an adsorbed Cl. The formation reaction is then the following:

$$SiCl_2^* + 2Cl^* \rightarrow SiCl_4 \quad (6)$$

The first route of the TCS formation mechanisms was repeated, with the same guessed intermediate state having all three atoms of the $SiCl_2$ molecule in a plane perpendicular to the surface. The resulting reaction pathway (see SI) had an activation barrier of 2.86 eV (65.95 kcal/mol), significantly higher than the barrier for TCS formation.

4. Current challenges and future research directions

In this study we attempted to find the minimum energy pathways for $SiCl_2$ and TCS molecule formation from bulk silicon atoms. However, as we noted in comparing the direct one step and indirect two-step paths for TCS formation, NEB is well suited to studying non-linear paths and inherently depends on simple interpolations and specification of final and initial states. A reasonable next step would be to explore other possible reaction pathways, such as routes with other intermediate species such as SiH and $SiCl_3$, through the use of more sophisticated techniques such as metadynamics. Furthermore, the coverage effect studies we conducted can be incorporated into a kinetic Monte Carlo model to produce more detailed kinetics suitable for use in analytic models. Similar studies should also be carried out on other silicon surfaces such as Si(111).

The effect of vacancies and surface defects should also be investigated, especially as surface dimers are depleted as in the case of $SiCl_2$ formation. We conducted an initial study in this direction when repeating the $SiCl_2$ formation reaction after removal of the first bulk atom. The energetics of the removal of subsequent Si (s) atoms would likely be affected, as would adsorption of molecules on the now distorted dimers. Another factor to consider is the use of catalysts for the chlorination/hydrochlorination system, where atomistic simulations of such systems have not been carried out. For example, Ding et al. [40] have proposed a mechanism for $CuCl_2$ catalyzed Si hydrochlorination which can further analyzed through theoretical simulations. Furthermore, MG-Si is known to have several impurities which are also thought to play a catalytic role and these could be also explored in future studies.

5. Conclusion

This paper sought to better understand mechanisms of silicon hydrochlorination used for the production of high purity silicon for use in solar photovoltaic or electronic applications. As part of this, we looked at the interaction of H_2, HCl, $SiCl_2$, dichlorosilane (SiH_2Cl_2 or DCS), trichlorosilane ($SiHCl_3$ or TCS) and silicon tetrachloride ($SiCl_4$ or STC) with the Si(100)-c(4 × 2) surface which is considered the most stable high temperature reconstruction of the most stable silicon surface.

First, the adsorption ability of single molecules was tested. The two diatomic molecules, H_2 and HCl, were found to dissociatively adsorb when placed directly over surface dimers. The latter was also found to dissociatively adsorb across two parallel dimers in an interdimer mechanism when placed between two parallel dimers. The $SiCl_2$ molecule dissociatively adsorbed between two parallel dimers in an interdimer mechanism when placed parallel to the surface and over a dimer or in the space between rows of parallel dimers. The molecule also strongly adsorbed, without dissociation but with strongest binding energy, when placed over the top of a dimer and perpendicular to the surface in an intradimer mechanism. Similarly, it strongly adsorbed without dissociating when placed between two parallel dimers in an interdimer mechanism.

The DCS, STC and TCS molecules dissociatively adsorbed through Si—Cl bond cleavage when placed over a dimer (splitting into a Cl atom adsorbed to one Si atom of the dimer and the remaining atoms adsorbed to the other Si atom of the dimer through the molecule's center Si atom). They did so with similar binding energies but this only occurred when the molecules were aligned with their Si—Cl bond parallel and directly above the dimer and close to the surface; in most other orientations the molecules moved away from the surface.

The effects of surface coverage were considered next by first decreasing coverage by doubling of the simulation supercell (the original supercell consisted of four surface dimers). The H_2 and HCl molecules did not display significant changes in binding energies while $SiCl_2$ and STC both decreased in binding energy, indicating that the latter two experienced stabilization through interaction of neighboring molecules. The coverage was then increased by adding additional molecules into the supercell. While a second H_2 molecule did not adsorb, three additional HCl molecules could be adsorbed to give complete coverage. This indicates the HCl molecules are very favorable to adsorb onto the surface and each additional molecule still produced very similar binding energies, thus indicating that inter-molecular interaction is not a significant factor for HCl.

Several configurations of two $SiCl_2$ molecules were tested, with a second molecule always adsorbing with stronger binding energy and resulting in a more stable system. The most favorable case was found to be when two $SiCl_2$ molecules were each placed over one of two parallel dimers, whereby the molecules rearranged themselves to form a surface complex. The addition of a second STC molecule still produced dissociative adsorption with a slight decrease in average binding energy but no ability to adsorbed additional molecules.

Finally, the removal of surface Si (s) to gas phase as part of the hyrochlorination reaction was investigated through reaction pathway analysis. The most favorable path was theorized to occur through $SiCl_2$ as an intermediate species. The formation of $SiCl_2$ from a surface dimer Si (s) atom and adsorbed Cl atoms was found to have a reaction barrier of 3.62 eV (83.48 kcal/mol), going down to 3.10 eV (71.49 kcal/mol) for a subsequent $SiCl_2$ formation. The formation of TCS from this $SiCl_2$ and adsorbed H and Cl atoms, where the TCS desorbs from the surface, was found to have a reaction barrier of 1.07 eV (24.68 kcal/mol). The formation of STC from this $SiCl_2$ was found to have a barrier of 2.86 eV (65.95 kcal/mol). A direct formation of desorbed TCS from a bulk Si atom was found to have a barrier of 4.92 eV (113.46 kcal/mol).

Acknowledgments

The authors would like to thank Natural Sciences and Engineering Research Council of Canada (NSERC), Mitacs and the University of Toronto in providing funding support for this work. The Atomsk [41], VESTA [42] and XCrysDen [43] open source software packages were invaluable in working with and visualizing the atomic systems.

Appendix A. Supplementary material

Supplementary data associated with this article can be found, in the online version, at https://doi.org/10.1016/j.apsusc.2018.12.253.

References

[1] A. Pandey, V. Tyagi, J.A. Selvaraj, N. Rahim, S. Tyagi, Recent advances in solar photovoltaic systems for emerging trends and advanced applications, Renew. Sustain. Energy Rev. 53 (2016) 859–884, https://doi.org/10.1016/j.rser.2015.09.043 http://www.sciencedirect.com/science/article/pii/S1364032115010138.

[2] G. Bye, B. Ceccaroli, Solar grade silicon: technology status and industrial trends, Sol. Energy Mater. Sol. Cells 130 (2014) 634–646, https://doi.org/10.1016/j.

solmat.2014.06.019.
[3] S. Yadav, K. Chattopadhyay, C.V. Singh, Solar grade silicon production: a review of kinetic, thermodynamic and fluid dynamics based continuum scale modeling, Renew. Sustain. Energy Rev. 78 (Supplement C) (2017) 1288–1314, https://doi.org/10.1016/j.rser.2017.05.019 http://www.sciencedirect.com/science/article/pii/S1364032117306494.
[4] M.D. Su, H.B. Schlegel, An ab initio MO study of the thermal decomposition of chlorinated monosilanes, SiH4-nCln (n = 0-4), J. Phys. Chem. 97 (39) (1993) 9981–9985, https://doi.org/10.1021/j100141a015 http://pubs.acs.org/doi/abs/10.1021/j100141a015.
[5] M.T. Swihart, R.W. Carr, Thermochemistry and thermal decomposition of the chlorinated disilanes ($Si_2H_nCl_{6-n}$, n = 0-6) studied by ab initio molecular orbital methods, J. Phys. Chem. A 101 (40) (1997) 7434–7445, https://doi.org/10.1021/jp971651t arXiv:arXiv:1011.1669v3, URL http://doi.wiley.com/10.1002/kin.550220606 . http://link.springer.com/10.1134/S003602440902006X .http://link.springer.com/10.1007/BF02502944 . https://doi.org/10.1016/j.tsf.2009.01.118 . http://ebooks.cambridge.org/ref/id/CBO9781107415324A009 . http://pubs.acs.org/doi/abs/10.1021/jp971651t.
[6] M.T. Swihart, R.W. Carr, On the mechanism of homogeneous decomposition of the chlorinated silanes. Chain reactions propagated by divalent silicon species, J. Phys. Chem. A 102 (9) (1998) 1542–1549, https://doi.org/10.1021/jp973174k URL < Go to ISI > ://WOS:000072305400014.
[7] J.M. Wittbrodt, H.B. Schlegel, An ab initio study of the thermal decomposition of dichlorosilane, Chem. Phys. Lett. 265 (3) (1997) 527–531, https://doi.org/10.1016/S0009-2614(96)01461-3 http://www.sciencedirect.com/science/article/pii/S0009261496014613.
[8] Q. Zhang, S. Wang, Y. Gu*, Direct ab initio dynamics studies of the reactions of h with sih4-ncln (n = 1-3), J. Phys. Chem. A 106 (15) (2002) 3796–3803, https://doi.org/10.1021/jp0140623.
[9] K. Pei, H. Li, *Ab initio* and kinetic calculations for the reactions of Cl with SiH_n Cl_{4-n} (n = 1,2,3,4), J. Chem. Phys. 121 (14) (2004), https://doi.org/10.1063/1.1788651.
[10] X. Zhang, Y.-h. Ding, Z.-s. Li, X.-r. Huang, C.-c. Sun, Ab initio study on the rate constants of SiCl4 + h [rightward arrow] SiCl3 + HCl, Phys. Chem. Chem. Phys. 3 (2001) 965–969, https://doi.org/10.1039/B006856J.
[11] S.P. Walch, C.E. Dateo, Thermal decomposition pathways and rates for silane, chlorosilane, dichlorosilane, and trichlorosilane, J. Phys. Chem. A 105 (10) (2001) 2015–2022, https://doi.org/10.1021/jp003559u http://pubs.acs.org/doi/abs/10.1021/jp003559u.
[12] S.P. Walch, C.E. Dateo, Reactions of SiCl2 and sihcl with H and Cl atoms, J. Phys. Chem. A 106 (12) (2002) 2931–2934, https://doi.org/10.1021/jp0126154.
[13] J. Deng, K. Su, X. Wang, Q. Zeng, L. Cheng, Y. Xu, L. Zhang, Thermodynamics of the gas-phase reactions in chemical vapor deposition of silicon carbide with methyltrichlorosilane precursor, Theoret. Chem. Acc. 122 (1) (2008) 1–22, https://doi.org/10.1007/s00214-008-0478-8.
[14] Y. Ge, M.S. Gordon, F. Battaglia, R.O. Fox, Theoretical study of the pyrolysis of methyltrichlorosilane in the gas phase. 3. Reaction rate constant calculations, J. Phys. Chem. A 114 (6) (2010) 2384–2392, https://doi.org/10.1021/jp911673h.
[15] T. Junko, M. Takamasa, S. Tadamasa, Thermal rate constants for SiH4 SiH3 + H and CH4 CH3 + H by canonical variational transition state theory, Bull. Chem. Soc. Jpn. 67 (1) (1994) 74–85, https://doi.org/10.1246/bcsj.67.74 http://www.journal.csj.jp/doi/pdf/10.1246/bcsj.67.74 http://www.journal.csj.jp/doi/abs/10.1246/bcsj.67.74.
[16] X. Yu, S.-M. Li, Z.-S. Li, C.-C. Sun, Direct ab initio dynamics studies of the reaction paths and rate constants of hydrogen atom with germane and silane, J. Phys. Chem. A 104 (40) (2000) 9207–9212, https://doi.org/10.1021/jp0004314.
[17] K. Matsumoto, .StephenJ. Klippenstein, . Kenichi Tonokura, M. Koshi, Channel specific rate constants relevant to the thermal decomposition of disilane, J. Phys. Chem. A 109 (22) (2005) 4911–4920, https://doi.org/10.1021/jp044121n pMID: 16833838.
[18] A.V. Vorotyntsev, S.V. Zelentsov, V.M. Vorotyntsev, Quantum chemical simulation of silicon tetrachloride hydrogenation, Russ. Chem. Bull. 60 (8) (2011) 1531–1536, https://doi.org/10.1007/s11172-011-0228-2 http://link.springer.com/10.1007/s11172-011-0228-2.
[19] S. Ravasio, M. Masi, C. Cavallotti, Analysis of the gas phase reactivity of chlorosilanes, J. Phys. Chem. A 117 (25) (2013) 5221–5231, https://doi.org/10.1021/jp403529x pMID: 23731215.
[20] Y. Ran, J.-B. Wang, Y.-X. Yin, Theoretical study on the SiH4-nCln (n = 0–4) reaction mechanisms for polysilicon production process, Comput. Theoret. Chem. 1035 (2014) 60–67, https://doi.org/10.1016/j.comptc.2014.02.031 http://linkinghub.elsevier.com/retrieve/pii/S2210271X14001029.
[21] A. Dkhissi, M.F. Reyniers, G.B. Marin, A theoretical study of standard heat of formation of systems involving in the zinc reduction of silicon tetrachloride, Theoret. Chem. Acc., 134 (1). doi:https://doi.org/10.1007/s00214-014-1593-3.
[22] M.A. Hall, C. Mui, C.B. Musgrave, DFT study of the adsorption of chlorosilanes on the Si(1 0 0)-2 × 1 surface, J. Phys. Chem. B 105 (48) (2001) 12068–12075, https://doi.org/10.1021/jp0118874.
[23] A. Barbato, C. Cavallotti, Challenges of introducing quantitative elementary reactions in multiscale models of thin film deposition, Phys. Status Solidi (B) Basic Res. 247 (9) (2010) 2127–2146, https://doi.org/10.1002/pssb.200945454.
[24] C. Cavallotti, Reactivity of silicon surfaces in the presence of adsorbed hydrogen and chlorine, Chem. Vap. Deposition 16 (10-12) (2010) 329–335, https://doi.org/10.1002/cvde.201006870.
[25] N. Kunioshi, K. Anzai, H. Ushijima, A. Fuwa, Effects of cluster size on calculation of activation energies of silicon surface reactions with H2 and HCl, J. Cryst. Growth 418 (2015) 115–119, https://doi.org/10.1016/j.jcrysgro.2015.02.068 http://linkinghub.elsevier.com/retrieve/pii/S002202481500158X.
[26] K. Anzai, N. Kunioshi, A. Fuwa, Analysis of the dynamics of reactions of SiCl 2 at Si (1 0 0) surfaces, Appl. Surf. Sci. 392 (2017) 410–417, https://doi.org/10.1016/j.apsusc.2016.09.039 http://linkinghub.elsevier.com/retrieve/pii/S0169433216319079.
[27] G. Valente, C. Cavallotti, M. Masi, S. Carrá, Reduced order model for the cvd of epitaxial silicon from silane and chlorosilanes, J. Cryst. Growth 230 (1) (2001) 247–257, https://doi.org/10.1016/S0022-0248(01)01349-5 proceedings of the Third International Workshop om Modeling in Crystal Growth. http://www.sciencedirect.com/science/article/pii/S0022024801013495.
[28] P. Gupta, P.A. Coon, B.G. Koehler, S.M. George, Adsorption and desorption kinetics for sicl4 on si(111)7 × 7, J. Chem. Phys. 93 (4) (1990) 2827–2835, https://doi.org/10.1063/1.458868.
[29] C.-S. Guo, K. Hermann, Y. Zhao, Dynamics and energetics of reconstruction at the si (1 0 0) surface, J. Phys. Chem. C 118 (44) (2014) 25614–25619, https://doi.org/10.1021/jp509095t.
[30] S. Back, J.A. Schmidt, H. Ji, J. Heo, Y. Shao, Y. Jung, On the structure of si(1 0 0) surface: importance of higher order correlations for buckled dimer, J. Chem. Phys. 138 (20) (2013) 204709, https://doi.org/10.1063/1.4807334.
[31] P. Giannozzi, S. Baroni, N. Bonini, M. Calandra, et al., Quantum espresso: a modular and open-source software project for quantum simulations of materials, J. Phys.: Condens. Matter 21 (39) (2009) 395502, https://doi.org/10.1088/0953-8984/21/39/395502.
[32] G. Kresse, D. Joubert, From ultrasoft pseudopotentials to the projector augmented-wave method, Phys. Rev. B 59 (1999) 1758–1775, https://doi.org/10.1103/PhysRevB.59.1758 http://link.aps.org/doi/10.1103/PhysRevB.59.1758.
[33] J.P. Perdew, K. Burke, M. Ernzerhof, Generalized gradient approximation made simple, Phys. Rev. Lett. 77 (1996) 3865–3868, https://doi.org/10.1103/PhysRevLett.77.3865 http://link.aps.org/doi/10.1103/PhysRevLett.77.3865.
[34] H.J. Monkhorst, J.D. Pack, Special points for brillouin-zone integrations, Phys. Rev. B 13 (1976) 5188–5192, https://doi.org/10.1103/PhysRevB.13.5188 http://link.aps.org/doi/10.1103/PhysRevB.13.5188.
[35] G. Mills, H. Jonsson, G.K. Schenter, Reversible work transition state theory: application to dissociative adsorption of hydrogen, Surf. Sci. 324 (1995) 305–337.
[36] H. Jónsson, G. Mills, K.W. Jacobsen, Nudged Elastic Band Method for Finding Minimum Energy Paths of Transition, World Scientific, 1998 pp. 385–404 (Chapter 16).
[37] G. Henkelman, H.G. Jonsson, Improved tangent estimate in the nudged elastic band method for finding minimum energy paths and saddle points, J. Chem. Phys. 113 (2000) 9978.
[38] A.H. Larsen, J.J. Mortensen, J. Blomqvist, I.E. Castelli, R. Christensen, M. Dułak, J. Friis, M.N. Groves, B. Hammer, C. Hargus, et al., The atomic simulation environment—a python library for working with atoms, J. Phys.: Condens. Matter 29 (27) (2017) 273002.
[39] I.Y. Zhang, J. Wu, X. Xu, Extending the reliability and applicability of b3lyp, Chem. Commun. 46 (2010) 3057–3070, https://doi.org/10.1039/C000677G.
[40] W.-j. Ding, Z.-b. Wang, J.-m. Yan, W.-d. Xiao, CuCl-catalyzed hydrogenation of silicon tetrachloride in the presence of silicon: mechanism and kinetic modeling, Ind. Eng. Chem. Res. 53 (43) (2014) 16725–16735, https://doi.org/10.1021/ie503242t http://pubs.acs.org/doi/abs/10.1021/ie503242t.
[41] P. Hirel, Atomsk: a tool for manipulating and converting atomic data files, Comput. Phys. Commun. 197 (Supplement C) (2015) 212–219, https://doi.org/10.1016/j.cpc.2015.07.012 http://www.sciencedirect.com/science/article/pii/S0010465515002817.
[42] K. Momma, F. Izumi, *VESTA3* for three-dimensional visualization of crystal, volumetric and morphology data, J. Appl. Crystallogr. 44 (6) (2011) 1272–1276, https://doi.org/10.1107/S0021889811038970.
[43] A. Kokalj, Computer graphics and graphical user interfaces as tools in simulations of matter at the atomic scale, Comput. Mater. Sci. 28 (2) (2003) 155–168, https://doi.org/10.1016/S0927-0256(03)00104-6 proceedings of the Symposium on Software Development for Process and Materials Design. http://www.sciencedirect.com/science/article/pii/S0927025603001046.